Scientia Iranica, Vol. 8, No. 2, pp 138–144

SCIENTIA
IRANICA

Analysis of Planar Anisotropic Sheet Metal Forming by the Finite Element Method

M. Foroutan*, M. Farzin[1] and H. Hashemolhosseini[1]

In this paper, the effects of planar anisotropy during some of the sheet metal forming processes are modeled using finite element method. Large deformation theory is applied and a rigid nonlinear hardening material is assumed. The virtual work principle is used and Lagrangian strains are considered in the definition of effective strain increment. Hill theory is used for modeling of anisotropy and the rotation of principal directions of anisotropy, due to large deformation, is also taken into consideration. A few complex examples are analyzed by introducing a relatively simple algorithm.

INTRODUCTION

Sheet metal forming is an important manufacturing process, widely used for a different range of products from beverage cans to auto-body parts to lightweight airframe and military aerospace components. There are two primary goals for the engineering analyses of sheet metal forming processes. First, analyses aim to reduce trial and error in the tooling and process design and, thereby, reducing material waste and leading to production of new parts. The second goal is to influence the design of desired parts for ease of manufacture. Both of these goals ultimately lead toward the objective of faster production of better parts at minimum cost.

A planar anisotropic sheet metal has a variety of mechanical properties in different directions, which are usually caused by rolling. Earring phenomenon in deep drawing process is caused by planar anisotropy. Therefore, its effects cannot be simply ignored in the analyses of sheet metal forming processes. Planar anisotropy has been considered by a number of researchers. In 1989, Kobayashi et al simulated the in-plane deformation of bore expanding and flange drawing processes using Hill theory [1]. In 1995, Hayashida et al. simulated punch stretching and cup drawing tests, using a new yield function developed by Barlet et al [2] and the ABAQUS/EXPLICIT code [3]. In the above mentioned research, rotation of the principal directions of anisotropy has been ignored. In 1995, Logan modeled the cup drawing process using both Hill quadratic yield criterion and Hosford non quadratic criterion, by the explicit finite element code DYNA3D [4]. In his analysis, he assumed that axes of principal stress and strain coincide, although for planar anisotropy they normally do not. In 1986, Yang and Kim [5] used a complex convective coordinate system to develop an F.E.M. program to handle planar anisotropic behavior and simulated rectangular bulge test and in-plane flange drawing. In the present work, it is assumed that the angle between the principal directions of anisotropy and the principal directions of strains remain constant during deformations at each point of the sheet. The above assumption is also applied by Yang and Kim [5]. The authors have modified the formulation introduced by Toh and Kobayashi for planar anisotropic material, which is a much simpler algorithm than Yang and Kim's procedure. In the present work, three different sheet metal forming processes are modeled. Firstly, stretching of narrow strips cut in different directions by a hemispherical punch is modeled. Secondly, the bore expanding test by a flat cylindrical punch is simulated. Finally, deep drawing of a circular blank by a hemispherical punch is modeled.

GOVERNING EQUATIONS

According to virtual work principle:

$$\int_{\nu} \bar{S}\delta(d\bar{E})d\nu - \int_{s} \underline{f}.\delta(\underline{u})ds = 0, \qquad (1)$$

where $\bar{S}$, $d\bar{E}$ and $\underline{f}$ are effective stress, effective strain increment and surface traction vector, respectively.

*. *Corresponding Author, Department of Mechanical Engineering, Razi University, Kermanshah, I.R. Iran.*
1. *Department of Mechanical Engineering, Razi University, Kermanshah, I.R. Iran.*

Due to the large deformation encountered, Lagrangian strains are used. The effective stress and strain increment in Hill theory for the state of plane stress are defined as follows [6]:

$$\bar{S} = \sqrt{\frac{3}{2}}\Big(\frac{FS_y^2 + GS_x^2 + H(S_x - S_y)^2}{F+G+H} + \frac{2NS_{xy}^2}{F+G+H}\Big)^{\frac{1}{2}}, \quad (2)$$

and:

$$d\bar{E} = \sqrt{\frac{2}{3}}\Big(\frac{(F+H)dE_x^2 + (H+G)dE_y^2}{FG+GH+FH} + \frac{2HdE_xdE_y}{FG+GH+FH} + \frac{2dE_{xy}}{N}\Big)^{\frac{1}{2}}. \quad (3)$$

In the above equations, x and y are principal directions of anisotropy. These directions are parallel and transverse to rolling direction, respectively, before deformation of the sheet. F, G and H are anisotropic coefficients. Ratios of these coefficients are assumed to be constant during deformations. In these simulations, rotations of principal axes of anisotropy are considered. It is assumed that the angle between principal directions of anisotropy and principal directions of strains remain unchanged. This rule is used to obtain principal directions of anisotropy at the end of each step. The principal directions of strains are calculated at the end of each step using Sowerby method [7].

It should be noted that in the above relations, the anisotropic coefficients do not need to be known and only their ratios F/H, G/H and N/H are sufficient. If the ratio of width strain to thickness strain in simple tension for strips cut into rolling direction and 45 and 90 degrees to the rolling direction are defined by R, Q and P, respectively, then according to Hill theory:

$$\frac{F}{H} = \frac{1}{P},$$
$$\frac{G}{H} = \frac{1}{R},$$
$$\frac{N}{H} = \frac{1}{2}\Big(\frac{1}{P} + \frac{1}{R}\Big)(2Q+1).$$

Therefore, these ratios can be evaluated by three simple tension tests.

The constitutive equation used in this model is assumed to be:

$$\bar{\sigma} = k\bar{\varepsilon}^n$$

For relating effective natural strain and Lagrangian strain, definition of plastic work is used:

$$\int \bar{S}d\bar{E} = \int \bar{\sigma}d\bar{\varepsilon}.$$

On the other hand, at any point:

$$\bar{\sigma} = \bar{\sigma}_0 + hd\bar{\varepsilon},$$

$$\bar{S} = \bar{S}_0 + Hd\bar{E},$$

where h and H are slopes of $\bar{\sigma}-\bar{\varepsilon}$ and $\bar{S}-\bar{E}$ constitutive curves, respectively, at a specific point. It is assumed that:

$$\bar{\sigma}_0 = \bar{S}_0,$$

therefore, it can be shown that:

$$H = h - 2\bar{\sigma}_0.$$

Consequently, at each point, $\bar{S}$ can be calculated [8].

DISCRETIZATION

Discretization of the problem domain is done by triangular linear elements. Displacement vector in each element is related to nodal point displacement vectors as:

$$\underline{u} = \underline{N}\,\underline{\hat{u}},$$

where:

$$\underline{u} = [u, \nu, w]^T,$$

$$\underline{\hat{u}} = [u_1, \nu_1, w_1, ..., w_3]^T.$$

It should be noted that displacements u, ν and w are defined in principal directions of anisotropy. On the other hand, the global displacement vector at each element is related to vector $\underline{u}$ as:

$$\underline{u} = \underline{A}\,\underline{U},$$

where $\underline{A}$ is the transformation matrix and:

$$\underline{U} = [U, V, W]^T.$$

Using the above relations, virtual work principle is written as:

$$\int_\nu \bar{S}\delta(d\bar{E})d\nu - \int_s \delta(\underline{U})^T\underline{A}^T\underline{N}^T\underline{f}ds = 0. \quad (4)$$

The above equation must be valid for any virtual displacement. Therefore:

$$\int_\nu \bar{S}\frac{\partial(d\bar{E})}{\partial(\underline{U})}d\nu - \int_s \underline{A}^T\underline{N}^T\underline{f}ds = 0. \quad (5)$$

Now, vector $\underline{dE}$ is defined as:

$$\underline{dE} = [dE_x, dE_y, dE_{xy}]^T.$$

Then:

$$d\bar{E} = \left(\frac{2}{3}\underline{dE}^T \underline{D}\ \underline{dE}\right)^{\frac{1}{2}},$$

where elements of the matrix $\underline{D}$ are functions of R, Q and P. Using definitions of Lagrangian strains, vector dE is related to vector $\underline{u}$ as:

$$\underline{dE} = \underline{B}\ \underline{u}.$$

Finally, virtual work principle can be written as:

$$\int_\nu \frac{2}{3}\frac{\bar{S}}{d\bar{E}}\underline{A}^T(\underline{B}+\underline{B}_{,\underline{u}})^T\underline{D}\ \underline{B}\ \underline{A}\ \underline{U}d\nu - \int_s \underline{A}^T\underline{N}^T\underline{f}ds = 0, \quad (6)$$

where notation $\underline{B}_{,\underline{u}}$ denotes partial derivative of $\underline{B}$ with respect to $\underline{u}$.

RESULTS AND DISCUSSIONS

In this research, three different sheet metal forming processes are modeled. In all of the three processes, the constitutive equation of sheet metal is assumed to be:

$$\bar{\sigma} = 627420\bar{\varepsilon}^{0.24},$$

when stress is measured in kPa.

Strip Stretching

As the first example, stretching of narrow strips cut by a hemispherical punch into the rolling direction and 45 and 90 degrees to the rolling direction are modeled. In these models, parameters R, Q and P are assumed to be 1, 3 and 5, respectively, and coefficient of friction is assumed to be zero. The width of strips is 12.5 mm, radius of punch 50 mm and radius of die throat 53 mm. Since strips are narrow and friction is neglected, these modeled examples are similar to simple tension tests. According to the flow rule for a strip cut into rolling direction:

$$\frac{\varepsilon_1}{(1+R)} = \frac{-\varepsilon_w}{R} \rightarrow \frac{\varepsilon_1}{\varepsilon_w} = \frac{-(1+R)}{R} = -2,$$

and for a strip cut 90 degrees to rolling direction:

$$\frac{\varepsilon_1}{(1+P)} = \frac{-\varepsilon_w}{P} \rightarrow \frac{\varepsilon_1}{\varepsilon_w} = \frac{-(1+P)}{P} = -\frac{6}{5}.$$

Variations of different strains along the strips are shown in Figures 1 and 2. From these figures, it is obvious that the ratios of longitudinal strain to width strain are almost equal to the above expected values for all the positions along the strip (-2 and -6/5).

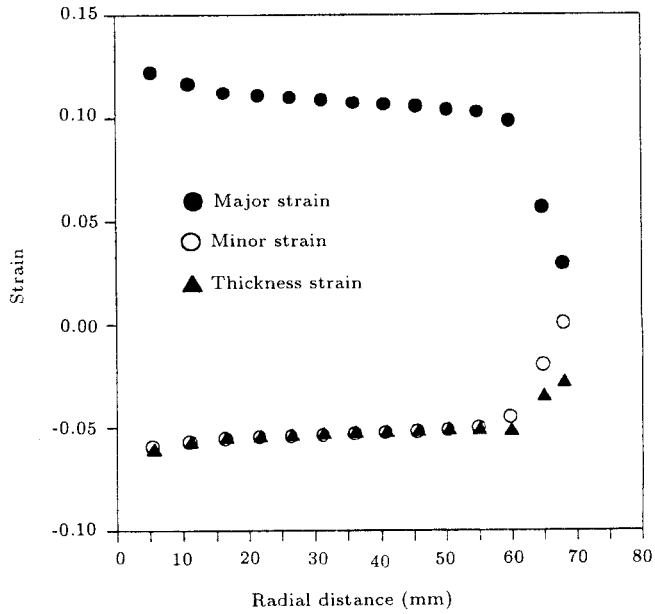

Figure 1. Strain distribution along rolling direction.

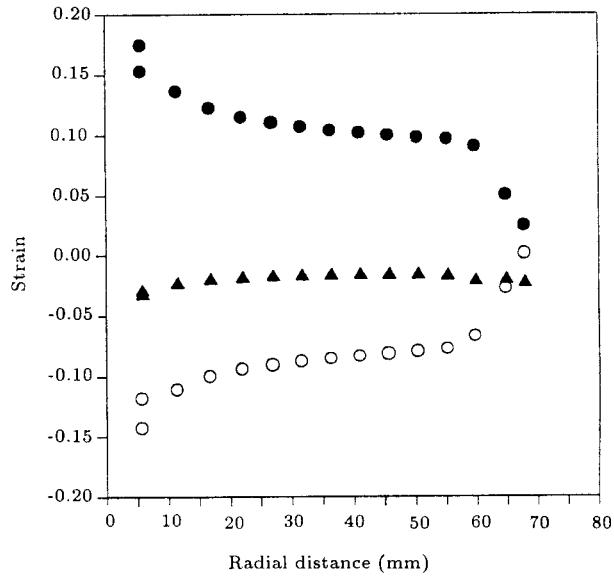

Figure 2. Strain distribution along 90 degrees to rolling direction.

Bore Expanding Test

As the second example, the bore expanding test is modeled. The geometry of forming tools is as follows. The punch is cylindrical with a 50 mm radius and shoulder radius of 10 mm. The die throat has a radius of 53 mm and the die corner radius is 5mm. Parameters R, Q and P are assumed to be 1, 3 and 1, respectively and coefficient of friction is assumed to be 0.2. In this case, a hole with a 10 mm radius is provided at the center of the blank. The effects of planar anisotropy are clearly seen from contours of major and thickness strains, shown in Figures 3 and

4. At the hole periphery, the radial stress is zero, therefore, the ratio of hoop strain to thickness strain can be calculated at this region. For the elements on global x and y axes, this ratio must be:

$$\frac{\varepsilon_h}{\varepsilon_t} = -(1+R) = -(1+P) = -2.$$

However, for the element on 45 degrees to global x axis:

$$\frac{\varepsilon_h}{\varepsilon_t} = -(1+Q) = -4.$$

Variations of major and thickness strains along the rolling direction and 45 and 90 degrees to the rolling direction are shown in Figures 5 and 6. These figures demonstrate that the above expected ratios are satisfactorily obtained by the presented model. A deformed mesh of this model is illustrated in Figure 7.

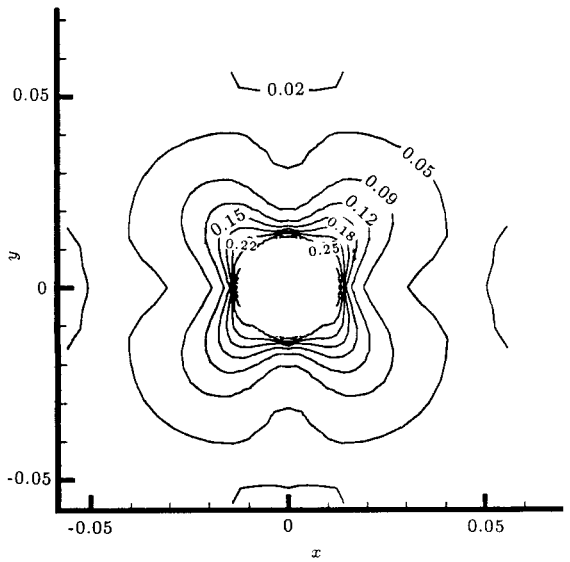

Figure 3. Contour of major strain for bore expanding.

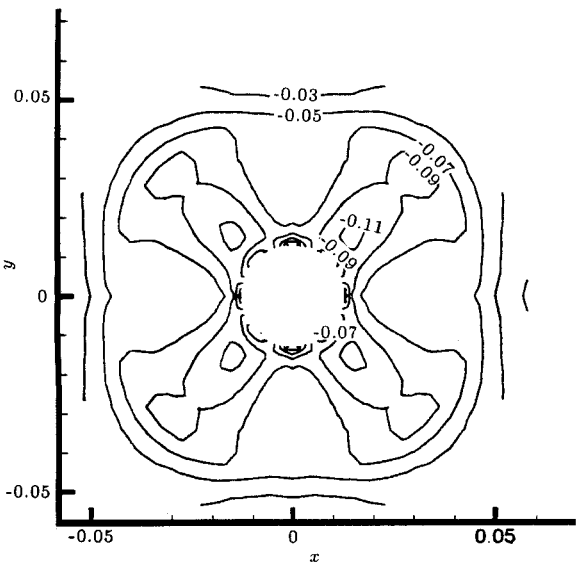

Figure 4. Contour of thickness strain for bore expanding.

Deep Drawing

Finally, deep drawing of a circular blank by a hemispherical punch is simulated. The radius of punch, die throat and die shoulder are assumed to be 30 mm, 31 mm and 8 mm and parameters R, Q and P are considered as 1, 3 and 1, respectively. The coefficient

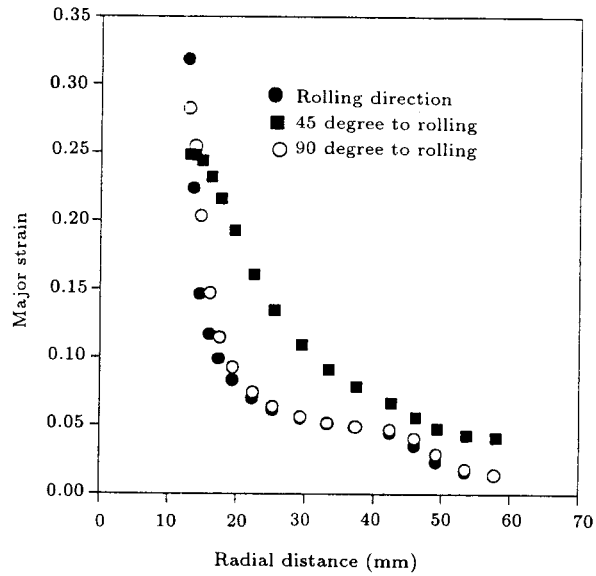

Figure 5. Major strain distribution for bore expanding.

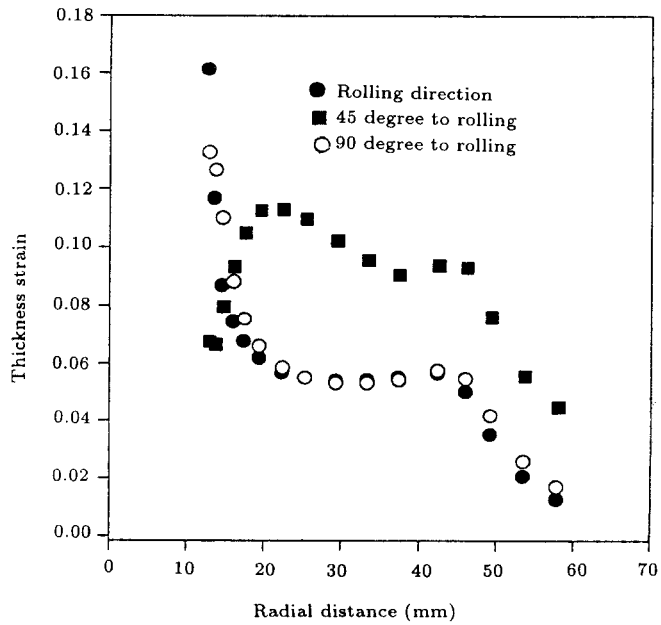

Figure 6. Thickness strain distribution for bore expanding.

of friction between punch and sheet is assumed to be 0.2 and between die and sheet is assumed to be 0.05. Deformed mesh of this model is shown in Figure 8, from which the effects of planar anisotropy are observed. Contours of major and thickness strains are illustrated in Figures 9 and 10. Variations of major and thickness strains along the rolling direction and 45 and 90 degrees to the rolling direction are shown in Figures 11 and 12. It is well-known that earring phenomenon in deep drawing processes is caused by planar anisotropy. In other words, although the initial blank is circular, in later stages of drawing processes, the periphery of the part does not remain circular. The rim thickness does not, also, remain uniform. From the results, it is realized that the thickness of the rim at 45 degrees to the rolling direction is smaller than the rolling and 90 degrees to the rolling directions.

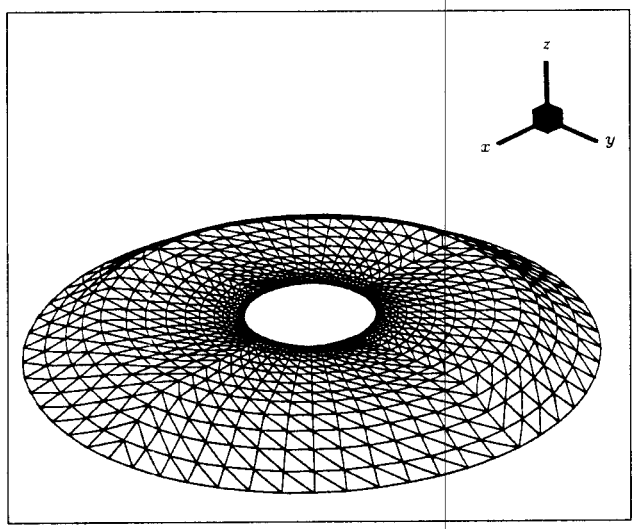

Figure 7. Deformed mesh for bore expanding.

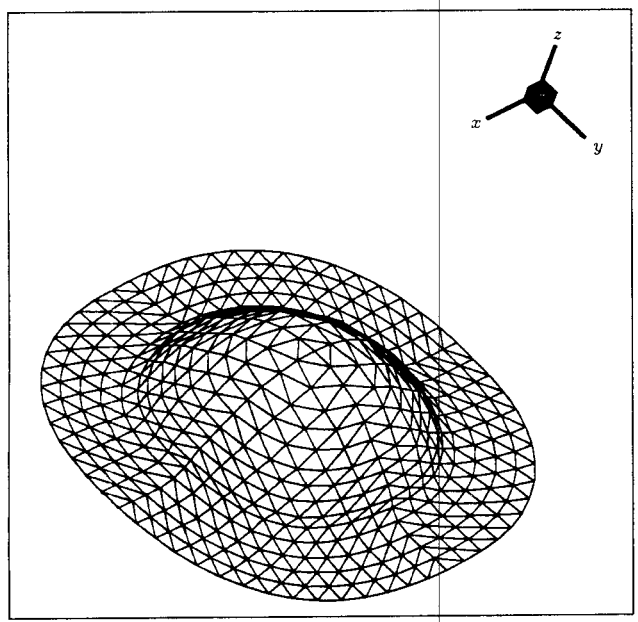

Figure 8. Deformed mesh for deep drawing.

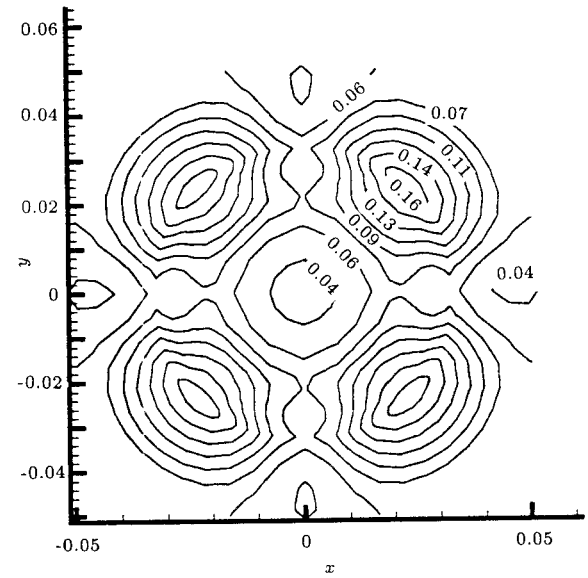

Figure 9. Contour of major strain for deep drawing.

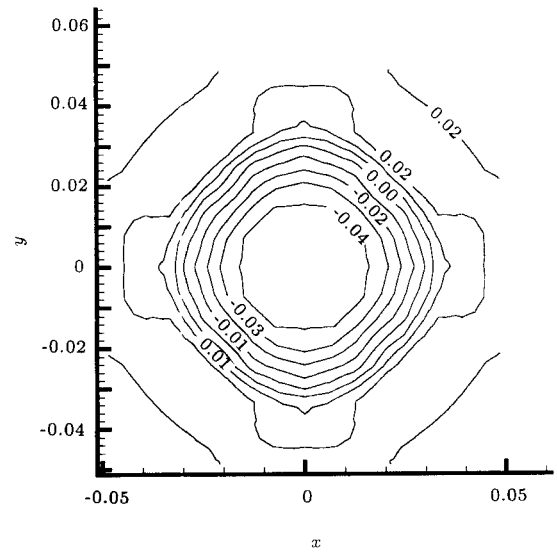

Figure 10. Contour of thickness strain for deep drawing.

On the contrary, the rim radius at 45 degrees to the rolling direction is greater than the rolling and 90 degrees to the rolling directions. The above predicted behaviors are well in agreement with experimental observations [9]. Assuming that stresses at the rim in the hoop, radial and thickness directions are $\bar{\sigma} : 0 : 0$, then from the flow rule, strain ratios at a specific point of the rim are as follows:

i) For an element on rolling direction or 90 degrees to rolling direction:

$$\frac{\varepsilon_h}{\varepsilon_t} = -(1+R) = -(1+P) = -2,$$

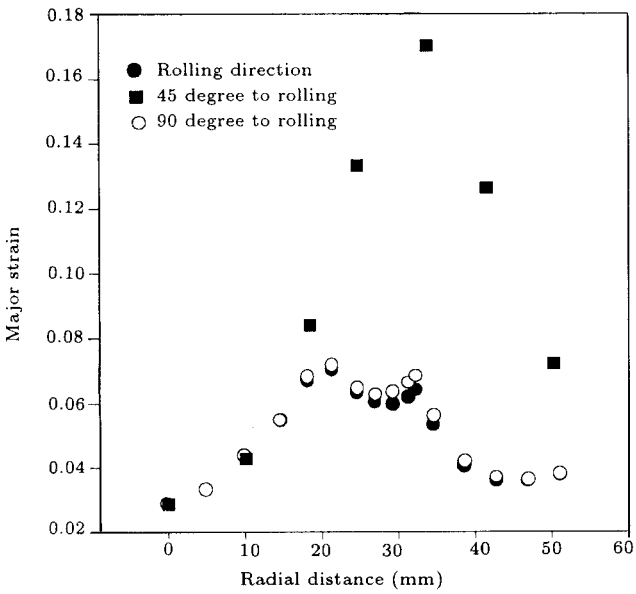

Figure 11. Major strain distribution for deep drawing.

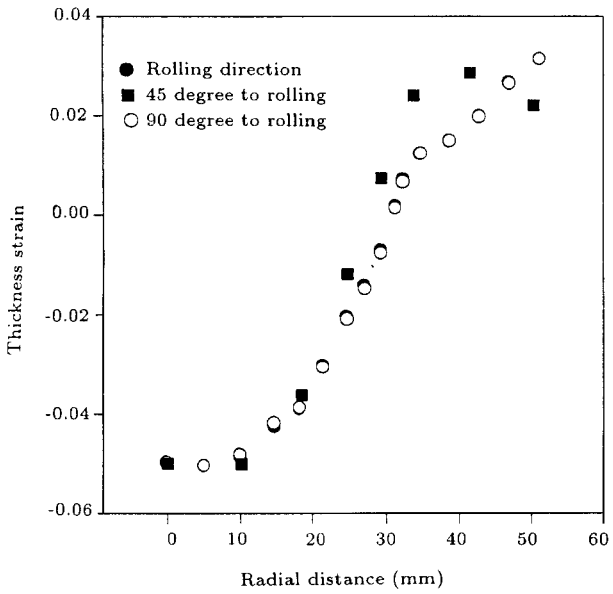

Figure 12. Thickness strain distribution for deep drawing.

ii) for an element 45 degrees to rolling direction:

$$\frac{\varepsilon_h}{\varepsilon_t} = -(1+Q) = -4.$$

From the results, it is also realized that the above relations hold between strain ratios at the mentioned points of the rim. In the present analysis, rotation of principal directions of anisotropy is also taken into account. For this purpose, at each step of calculations, principal directions of strains are determined with respect to local coordinates of elements. It is assumed that the angle between principal directions of strain and anisotropy remains constant in all stages

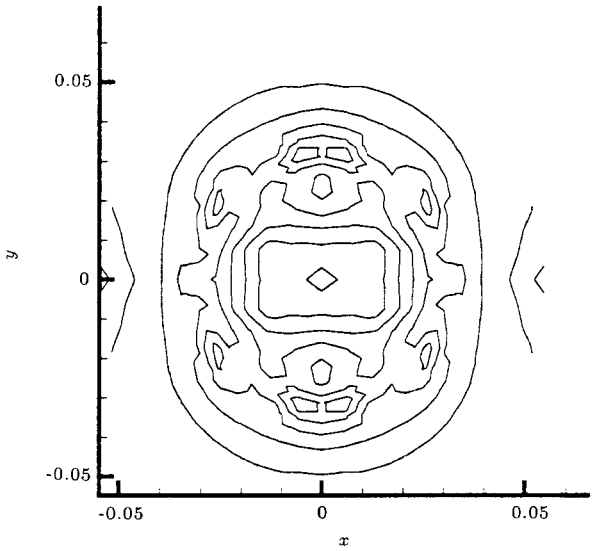

Figure 13. Contours of major strain for deep drawing without considering rotations.

of deformation at each point. Hence, new directions of anisotropy can be obtained with respect to local coordinates of each element. In Figure 13, contours of major strain are shown for a deep drawing process with the same above conditions except that the angle between principal directions of anisotropy and local coordinates of the elements are assumed to remain unchanged. In other words, rotations of principal directions of anisotropy are neglected. As can be seen, in this case, contours of major strains in rolling and 90 degrees to rolling directions are different, although the anisotropic parameters R and P are the same. For this particular deep drawing example, the maximum rotation of principal direction of anisotropy is about 10 degrees. Clearly, these rotations cannot be simply ignored and for obtaining better results they should be taken into consideration. However, for the strip stretching example, rotations are not so severe.

CONCLUSIONS

In this paper, three dimensional deformations of planar anisotropic sheet metal are simulated by finite element method. It is demonstrated that under different loading conditions such as strip stretching (simple tension), bore expanding (biaxial stretching) and deep drawing (biaxial tension and compression), effects of planar anisotropy on strain distributions can be obtained. It is also shown that under different loading conditions, the predicted values are in good agreement with physical reality. Occurrence of earring phenomenon during deep drawing is also illustrated for a circular blank. Rotations of principal directions of anisotropy are also taken into account, which under complex conditions

of loading such as deep drawing are considerable. Consequently, it is important to consider these factors for obtaining better results.

NOMENCLATURE

$\underline{A}$	transformation matrix
$\underline{B}$	matrix relating strain to displacements
$\underline{D}$	matrix relating strain vector to effective strain
$\underline{dE}$	Lagrangian strain increment vector
$d\bar{E}$	effctive Lagrangian strain increment
F, G, H	planar anisotropic coefficients
L, M, N	planar anisotropic coefficients
$\underline{f}$	surface traction vector
$\underline{N}$	matrix of shape functions
$\underline{U}$	displacement vector in global coordinates
$\underline{u}$	displacement vector in local coordinates
$\underline{\hat{u}}$	nodal displacement vector
R, Q, P	R-values in different directions of the sheet
S	second Piola-Kirchoff stress
$\bar{S}$	effective Piola-Kirchoff stress
ε	natural strain
$\bar{\varepsilon}$	effective natural strain
σ	Cauchy stress

REFERENCES

1. Kobayashi, S., *Finite Element Method in Metal Forming*, Oxford University (1986).
2. Hayashida, Y., Meada, Y., Hatsui, N., Hattori, S. and Yanagawa, M. "F.E.M. analysis of punch stretching and cup drawing tests for aluminum alloys using a planar anisotropy yield function", in *Simulation of Materials Processing Theory Methods and Applications*, Shen & Dawson, Eds., Balkem, Rotterdam, ISBN 9054105534 (1995).
3. Barlet, F., Lege, D.J. and Brem, J.C. "A six component yield function for anisotropic material", *Int. J. of Plasticity*, **7**, pp 693-712 (1991).
4. Logan, R.W. "Finite element analysis of earring, using non-quadratic yield surfaces", in *Simulations of Materials Processing Theory Methods and Applications*, Shen & Dawson, Eds., Balkem, Rotterdam, ISBN, 9054105534 (1995).
5. Yang, D.Y. and Kim, Y.J. "A rigid plastic finite element formulation for the analysis of general deformation of planar anisotropic sheet metal and its applications", *Int. J. of Mech. Sci.*, **28**(12), pp 825-840 (1986).
6. Hill, R., *Mathematical Theory of Plasticity*, Oxford University Press, London (1950).
7. Sowerby, R. , Chu, E. and Duncan, L., *J. Strain Analysis*, **7**, pp 95-101 (1982).
8. Toh, C.H. and Kobayashi, S. "Process modeling of sheet metal forming of general shapes by the F.E.M. based on large strain formulation", Ph.D Thesis , University of California, Berkeley (1983).
9. Farzin, M. "Deep drawing without a blank holder", M.Sc Dissertation, Dept. of Mech. Eng., UMIST, England (1983).